6-1-2020

An experimental study on micro-structural and geotechnical characteristics of expansive clay mixed with EPS granules

Nitin Tiwari

Neelima Satyam

Sanjay Kumar Shukla
Edith Cowan University, s.shukla@ecu.edu.au

10.1016/j.sandf.2020.03.012
Tiwari, N., Satyam, N., & Shukla, S. K. (2020). An experimental study on micro-structural and geotechnical characteristics of expansive clay mixed with EPS granules. Soils and Foundations, 60(3), 705 - 713). https://doi.org/10.1016/j.sandf.2020.03.012

HOSTED BY
ELSEVIER
Available online at www.sciencedirect.com
ScienceDirect
Soils and Foundations 60 (2020) 705–713
SOILS AND FOUNDATIONS
www.elsevier.com/locate/sandf

Technical Note

An experimental study on micro-structural and geotechnical characteristics of expansive clay mixed with EPS granules

Nitin Tiwari [a,*], Neelima Satyam [a], Sanjay Kumar Shukla [b,c]

[a] Discipline of Civil Engineering, Indian Institute of Technology Indore, Madhya Pradesh 452020, India
[b] Discipline of Civil and Environmental Engineering, School of Engineering, Edith Cowan University, Perth, Australia
[c] School of Building and Civil Engineering, Fiji National University, Suva, Fiji

Received 25 May 2019; received in revised form 5 March 2020; accepted 23 March 2020
Available online 25 May 2020

Abstract

Pavement structures constructed on the expansive soil subgrade experience a higher upward pressure compared to any other subgrade material. The upward pressure is caused due to high swelling and shrinkage characteristics of expansive clay soil. The present study has investigated and identified the mechanisms by which a remolded expansive soil can be modified to reduce the upward pressure and swelling (heave). To achieve this, a lightweight, environmentally friendly, and high pressure resistive expanded polystyrene (EPS) granules have been used with expansive soil s from three different locations of Madhya Pradesh state, India. The study has been performed to understand the swelling and strength characteristics of soil with and without the use of EPS (density = 21.6 kg/m^3) as per ASTM specifications. The chemical and microstructural components of the expansive soil were investigated using autotuned total reflectance Fourier transform infrared (ATR-FTIR), X-ray diffraction (XRD), and scanning electron microscope (SEM). Several laboratory experiments, including optimum moisture content, maximum dry unit weight, grain-size distribution, liquid limit, plastic limit, shrinkage limit, free swell index, unconfined compressive strength, and pressure swelling tests were carried out on the statically compacted expansive clay soil specimen with and without EPS (0.25%, 0.50%, 1.00%). The maximum addition of EPS was considered as 1% as the very high expansion was observed, and beyond this, further addition of EPS was not feasible. The results show that the swelling pressure, expansion percentage, and time rate of swell decrease, whereas the unconfined compressive strength (UCS) increases with the addition of EPS. The inclusion of EPS in expansive clay soil exponentially reduced the heave and the upward pressure, whereas the maximum UCS was observed at 0.5%.

Keywords: EPS; Expansive soil; Heave; Microstructural analysis; Swelling pressure; Unconfined compressive strength

1. Introduction

The construction of pavement structures plays an indispensable role in the socio-economic development of a country. The rapid development of pavement construction in India inevitably encounters the problematic situation of expansive soil subgrade. The unpredictable settlement of expansive soil subgrade is the most challenging task for geotechnical engineers. The expansive soil subgrade is usually considered unsuitable for supporting cyclic loads (Zhou et al., 2018). The expansive soil subgrade experience changes in volume and upward swelling pressure due to seasonal variation in moisture content. This variation can cause adverse effects on the paved structure constructed on expansive soil subgrade (Öncü and Bilsel, 2017; Puppala et al., 2006). Expansive soils undergo volumetric changes with variation in moisture content, and if it is not allowed to swell freely, then it causes upward swelling pressure on the resisting structure. If swelling pressure is

Peer review under responsibility of The Japanese Geotechnical Society.
* Corresponding author.
E-mail addresses: phd1801204006@iiti.ac.in (N. Tiwari), neelima.satyam@iiti.ac.in (N. Satyam), s.shukla@ecu.edu.au (S. Kumar Shukla).

https://doi.org/10.1016/j.sandf.2020.03.012
0038-0806/

not controlled, it may cause uplifting and distress of the structure (Nelson and Miller, 1993; Shelke and Murthy, 2010).

The expansive soils persuasively affect the construction activities in various parts of the United States, South America, Canada, Africa, Australia, Europe, India, and China (Khosrowshahi and Yildirim, 2014). In India, 15–20% of the surface deposits consist of expansive soil (Rao et al., 2001). The construction of pavements experiences extensive large-scale damage caused by swelling accompanied by loss of strength and shrinkage cracks during monsoon and summer, respectively (Srinivas et al., 2016). India has one of the most extensive road networks in the world, spanning over a total of 5.5 million km and 90% of India's passenger traffic use road network (MORTH, 2019). The World Health Organization report in 2018 indicated that the deaths caused due to road traffic crashes have increased to 1.25 million per year which is roughly 3700 people every day. The non-lucrative countries (24.1 deaths/100,000 population) having a 2.6 times higher death rate due to road traffic injuries than in lucrative countries (9.2 deaths/100,000 population) (World Health Statistics, 2018). The Ministry of Road Transport and Highway, India (MORTH) has declared over 4,64,910 road accidents. States and Union Territories (UTs) reported 147,913 lives and causing injuries to 470,975 peoples in the calendar year 2017 (MORTH, 2019).

In order to achieve a safe and sustainable structure, engineers should examine the use of alternative materials which would reduce the swelling shrinkage behaviour of expansive clay soil without affecting the construction schedule (Srivastava et al., 2018). Soil improvement is achieved by altering its mechanical and/or chemical properties. Chemical treatment mainly involves the inclusion of chemicals admixtures (e.g., polymers, cement, and lime) to the soil (Al-Rawas et al., 2005; Estabragh et al., 2014; Mirzababaei et al., 2009; Tatsuoka and Correia, 2016; Yazdandoust and Yasrobi, 2010) and mechanical approach includes the compaction of soil with the addition of the strengthening material. Common strengthening materials include synthetic fibres (e.g., nylon and polypropylene) (Phanikumar and Singla, 2016; Senol et al., 2014), natural fibres (e.g., coconut and coir) (Prusty and Patro, 2015; Sivakumar Babu et al., 2008; Tiwari and Satyam, 2020), geofoam (Aytekin, 1997a,b; Beju and Mandal, 2017) and rubber (Bekhiti et al., 2019) or other fibrous materials. The use of non-conventional lightweight geomaterials like EPS, polypropylene, rubber, has presented both opportunities and challenges to researchers and engineers worldwide (Bekhiti et al., 2019; Tiwari and Satyam, 2019; Zhou et al., 2018). The use of EPS-block geofoam has gained popularity due to its vast application areas such as compressible inclusion (Ghani et al., 2005; Horvath, 1994; Zarnani and Bathurst, 2007), reduction of swelling pressure caused by large subgrounds (Aytekin, 1997a,b), to fill materials in road excavations (Arellano and Stark, 2011) and remediation of sandy slopes (Akay et al., 2013). To overcome the limitations like transport problem, lack of formability to fill volumes and compatibility with in-situ soil EPS, lightweight padding material, a mixture of EPS grains with soil and alternative additives has been recommended (Karimpour-fard and Chenari, 2015; Liu et al., 2006; Yoonz et al., 2014). According to Horvath (1997), higher compressive behaviour of EPS can reduce swelling pressures and has several advantages to conventional methods of stabilization such as ease in construction, less time for construction, reduced immediate settlements and high durability.

The primary focus of this study has been to develop, characterize, and formulate a soil stabilization technique using EPS for the Indian road scenario, which is yet poorly studied. The swelling pressure can be determined by the swell consolidation method, different pressure method, and constant volume method. The experimental study carried out by Soundara and Robinson (2009) shows that in the constant volume method, the soil fabric remains the same and gives moderate swelling pressure. Constant volume swelling pressure test has been adopted to calculate the upward swelling pressure and expansion percentage. The stress-strain behaviour has been concluded by carrying out the unconfined compressive strength test.

2. Properties of material

2.1. Basic characteristics of soil

Three different expansive soils were collected from the Madhya Pradesh state of India at a depth of 1−1.5 m. The expansive soils considered for the study were referred to as BC-01, BC-02, and BC-03. The values of the free swelling index of the soil at 28 days were found to be 120%, 85%, and 60% for BC-01, BC-02, BC-03, respectively. These results show the different swelling potential of soils considered for the study. As per the unified soil classification system (USCS), soils were classified as highly plasticity clay (CH). The various index properties of the expansive soil considered are shown in Table 1.

Table 1
Index properties of expansive soil considered in the study.

Property	BC -1	BC -2	BC -3
Specific gravity	2.78	2.68	2.63
Liquid limit (%)	87	69.67	73.51
Plastic limit (%)	49	32.64	41.37
Plasticity index (%)	38	37.03	32.14
Shrinkage limit (%)	11	20.51	10.66
USCS soil classification	CH	CH	CH
Grain size distribution			
Clay (%)	71.5	63.50	57.20
Silt (%)	24.5	31.7	37.4
Sand (%)	4.0	4.80	5.40
Free swell index (%)	120	85	60
Optimum moisture content (%)	19.2	18.62	17.93
Maximum dry unit weight (kN/m^3)	17.65	17.79	18.02

2.2. Microstructural characteristics

The chemical and microstructural components of the all three expansive clayey soils were microscopically analyzed using the Fourier Transform Infrared (FTIR), X-ray Diffraction (XRD) and Scanning Electron Microscopy (SEM). The microstructural analysis of the clay soil was investigated to assess the mineralogy of the expansive soil and determine the responsible mineral for the swell shrinkage behavior of the soil present in the study area.

IR Spectral characterization of peat was performed using diamond-attenuated total reflectance Fourier Transform Infrared (ATR-FTIR) spectrometer (PerkinElmer) equipped with a potassium bromide beam splitter. The Diamond Attenuated Total Reflectance (DATR) accessory, with a single reflection system, was used to produce transmission spectra. The specimen was dehydrated by freeze-drying and powdered. The specimen was placed directly on a KRS-5 crystal, and a flat point powder press was used to achieve even distribution and contact. IR spectra were obtained by an average of 200 scans with a resolution of 4 cm^{-1} over the range of 4000–500 cm^{-1}. A correction was made to spectra for the ATR to allow differences in depth of beam penetration at different wavelengths. The IR spectra were also corrected for attenuation by water vapor and CO_2. Differences in the amplitude and baseline between the runs have corrected by normalizing the data by subtracting the specimen minimum followed by division by the average of all data points per specimen. The first and second derivatives were calculated to determine and test correlations of organic matter variables that formed 'shoulders' rather than individual peaks in the FTIR profiles.

The range of 500 cm^{-1} to 1200 cm^{-1} presented the presence of minerals, 1200 cm^{-1} to 3000 cm^{-1} organic matters, and 3500 cm^{-1} to 4000 cm^{-1} clay minerals (Robertson et al., 2013). The characteristic bands of 3382, 3432, 3552, 3600, 3610 and 3698 cm^{-1} represent the vibration (stretching) of the hydroxyl groups (OH) of illite and kaolinite (Farmer, 1974). The other bands at 1008, and 1104 cm^{-1} are those of Si-O bonds and the bands at 714 and 528 cm^{-1} arise from the deformation vibrations of Al^{IV}-OSi and Al^{VI}-OSi. The doublet peak at 798 and 782 cm^{-1} and a single peak located at 694 cm^{-1} can be attributed to the quartz vibrations (Criado et al., 2007). Also, the band located at 912 cm^{-1} can be attributed to the deformation vibration of Al-OH (Christelle, 2005). Kaolinite has been identified at a peak of 3698 and 798 cm^{-1} (Alvarez-Puebla et al., 2005; Mackenzie, 1957) and a third band observed at 3552 cm^{-1}, which correspond to the absorbance associated to ferric ions of kaolinite (Petit et al., 1999). The bands at 1634 cm^{-1} indicating to the vibration of adsorbed water molecules (angular deformation) between the layers (see Fig. 1).

Microstructure and morphology play an important role in the status of expansive soil and influence expanding and shrinking behavior (Corey, 2010). The freeze-cut-dying

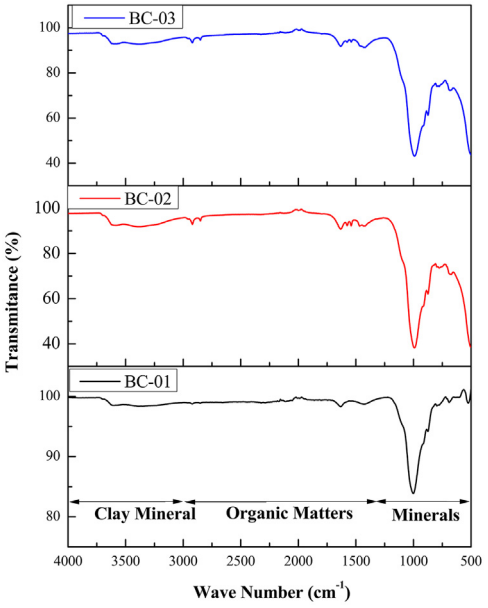

Fig. 1. IR spectra of expansive soil.

method is used for preparing the soil specimen for the microstructural analysis using SEM. This method can preserve the original soil microstructure and minimize flaws such as erroneous orientation and false void which occur in the SEM image (Shi et al., 1999). The obtained specimen was coated with the steel paste and then scanning electron microscopic images of the specimen were developed in the laboratory. The images obtained from the specimen was compared with the standard image of clay minerals.

The SEM micrograph as presented in Fig. 2(a) shows many cavities in the specimen which indicates the false void present in the soil. The SEM images presented in Fig. 2(b) shows irregular wavy edges of the particles and the flaky structure of montmorillonite (Atahu et al., 2019). Fig. 2 (d) shows the flat-lying plates typical of illite whereas Fig. 2(c) depicts expanded, flared, "cornflake" or "oak leaf" texture of Na-montmorillonite (Inoue et al., 1986).

The mineralogical characteristics of the expansive soil were translated using X-ray diffraction analysis (XRD). The analysis of the XRD pattern is shown in Fig. 3 and was obtained using the Pananalytical X'pert Highscore Plus software. X-ray diffraction analysis data shows the peak of quartz as a distinct peak. The position of 2θ at 20.86°, 21.98°, 26.64°, 39.42°, 50.1°, 59.94° and 67.96° match with the quartz spectra. The peaks located at 2θ of approximately 5.76°, 19.72°, 23.58°, and 27.68° are the peaks for the montmorillonite. The calcite has observed at the peak of 29.44°, 35.72°, 39.42° and 48.62° and Hematite at the peak of 24.42°, 35.72° and 39.42°. It was observed that 39.42° is the common peak for the quartz, hematite, and calcite, and the illite clay mineral diffraction peak was observed at 21.42°. The XRD results concluded that the quartz is present at higher amounts in expansive soil. However, the presence of montmorillonite, illite, hematite, and calcite was also observed.

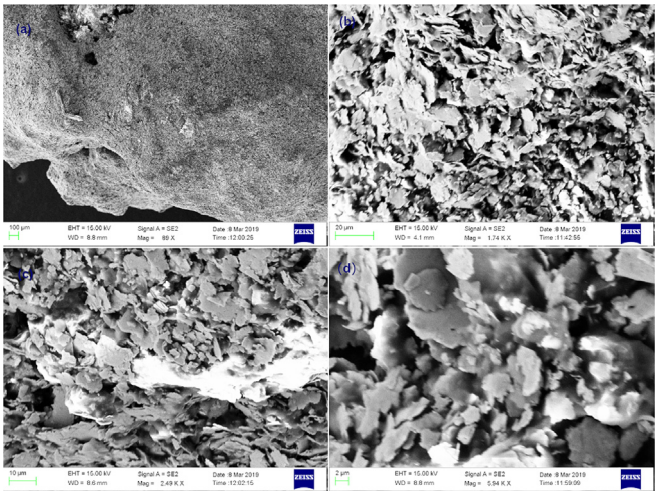

Fig. 2. SEM micrograph of expansive clay soil (a) 100 μm (b) 20 μm (c) 10 μm (d) 2 μm.

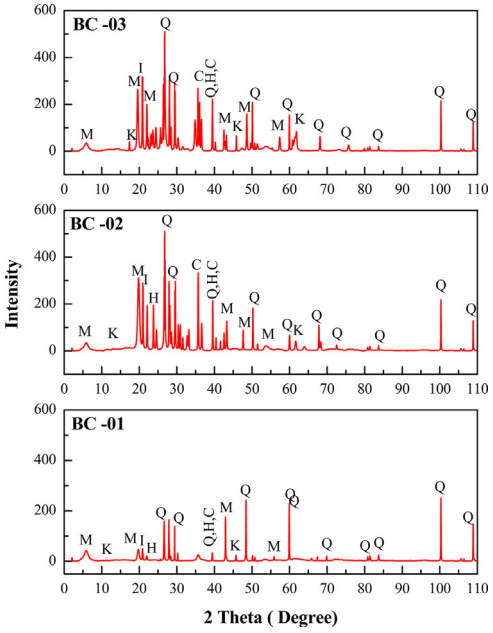

Fig. 3. XRD analysis of expansive soil.

2.3. Expanded polystyrene (EPS)

EPS is the macro-molecule polymer with prior light-weight properties. During the forming process of EPS granular, several individual pores are formed because of expanding of the blowing agent which results in an increase to volume by up to 40 times (Zhou et al., 2018). The EPS of density (21.6 kg/m^3) used in this study and was provided by Shree Insupac Geofoam, Mumbai, India. The low mass/volume ratio characteristic of the EPS is a significant problem in the disposal; hence, its utilization in construction can reduce the disposal problem of EPS waste. The properties of the EPS have been tested as per the ASTM standard. The properties of the EPS geofoam used in this study is mentioned in Table 2.

Table 2
Properties of EPS considered in the study.

Property	Value
Density (min.) (kg/m^3)	21.6
Compressive strength @ 1% deformation (kPa)	50
Compressive strength @ 5% Deformation (kPa)	115
Compressive strength @ 10% deformation (kPa)	135
Elastic modulus (min.) (kPa)	5000
Flexural strength (min.) (kPa)	276
Water absorption by total weight (max.) (%)	3.00
Oxygen index (min.) (%)	24.00
Buoyancy force (kg/m^3)	980

3. Experimental work

In the present work, several engineering properties of the clayey soil and EPSC mix were investigated. The three different expansive soils have been used in this study to present the EPS potential to control the swelling pressure and maintaining the unconfined compressive strength of reinforced expansive soils. The index properties of soils have been determined using Atterberg's limits, standard Proctor, free swell index, grain size distribution, and specific gravity test. Microstructural characterization of soils has been carried out by conducting XRD, FTIR and SEM analyses. To understand the swelling shrinkage behaviour of the expansive soil the constant pressure swelling test has been conducted for 28 days with the inclusion of 0.25%, 0.5%, and 1.00% EPS content by weight of dry soil. All the experiments were conducted three times to reduce the uncertainty in the results and to study the condition of repeatability. The initial moisture content and dry unit weight are essential factors affecting the swelling behaviours of expansive soil (Elsharief et al., 2014). Hence, the specimen was prepared at the dry unit weight and optimum moisture content of expansive soil. The dry mix of 4.75 mm sieved clayey soil (Bc-01, BC-02, BC-03) oven-dried at 105–110 °C and EPS (0.25%, 0.50% and 1.005 by weight of dry soil) was prepared and kept in environmental chamber at 27 ± 2 °C and 65 ± 5% humidity to maintain the constant temperature and moisture content in the soil mass. The EPS could not mix homogenously, and as a result, segregation and improper bond were observed because of the differences in unit weights and the lack of adhesion between the expansive soil and EPS. The required amount of clay and soil-EPS mixes were compact statically using a lightweight proctor to achieve the field conditions. The test specimens were prepared in accordance with IS:2720-1, 1983 (IS:2720-1, 1983). The prepared specimen (100 mm height and 10 mm diameter) of clay and EPSmix were tested for 28 days in the pressure swelling consolidation apparatus. The heave and the upward swelling pressure were noted at fixed duration in accordance with the IS: 2720-41, 1977. The inclusion of EPS may reduce the compressive strength of the clay due to segregation and improper bond and hence to analysis the variation of compressive strength of the expansive soil the UCS test conducted. The UCS specimen of 38 mm diameter with

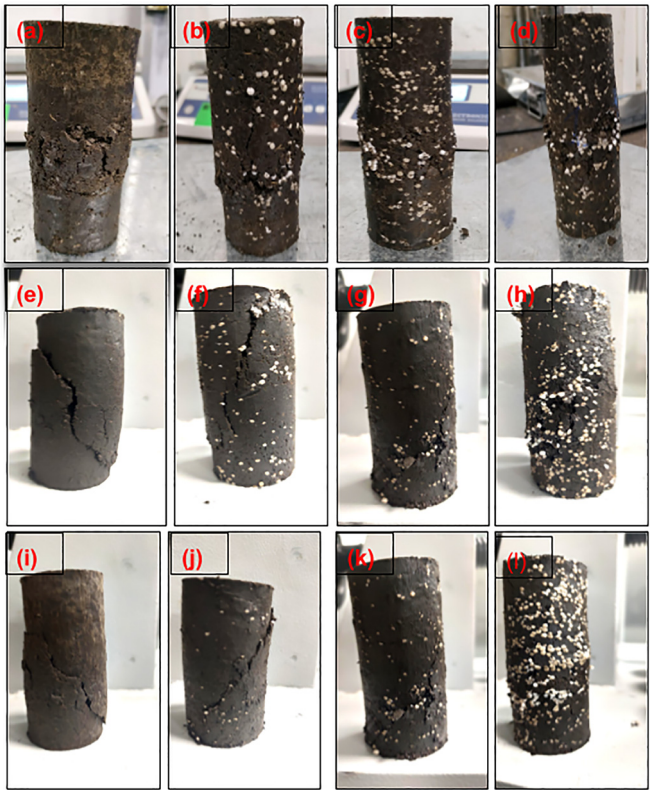

Fig. 4. UCS failure pattern of reinforced and unreinforced soil (a) BC-01 (b) BC-01 + 0.25% EPS (c) BC-01 + 0.50% EPS (d) BC-01 + 1.00% EPS (e) BC-02 (f) BC-02 + 0.25% EPS (g) BC-02 + 0.50% EPS (h) BC-02 + 1.00% EPS (i) BC-03 (j) BC-03 + 0.25% EPS (k) BC-03 + 0.50% EPS (l) BC-03 + 1.00% EPS.

maintaining the length depth ratio between 2 and 2.5 was prepared and placed in the environmental chamber at 27 ± 2 °C and 65 ± 5% humidity to maintain the constant temperature and moisture content. The clay and EPS mix specimens were tested at 1.25 mm/min strain rate and the values of vertical displacement and load carrying capacity has been recorded with 25 mm capacity LVDT and 50kN capacity load cell. The failure patterns of clay, 0.25%, 0.50%, and 1.00% EPSC are depicted in Fig. 4.

4. Results and discussion

The swelling pressure is defined as the pressure to maintain the volume of specimen constant while undergoing saturation in between two successive readings. The maximum swelling pressures of reinforced and unreinforced soils with varying percentages of EPS are shown in Fig. 5. This depicts that the swelling pressure decreases with an increase in EPS content except at 0.25% EPS content. It is because, in 0.25% EPS, the EPS is in very low concentration which creates a void in the soil. These voids, when filled with water exert higher initial pressure with time and the soil particles create a bond with the EPS beads, which leads the upward pressure to be constant. As the expansive soil is a visible indicator of swelling, its reduction with the addition of EPS is noticeable, as shown in Fig. 6. The reduction

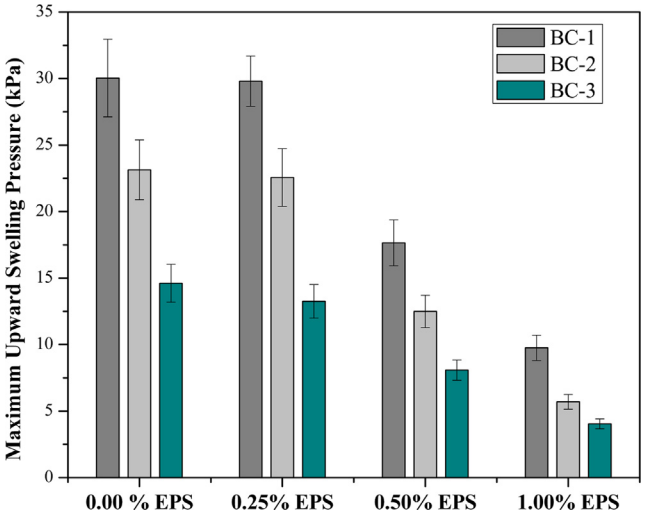

Fig. 5. Maximum swelling pressure of reinforced and unreinforced expansive soil.

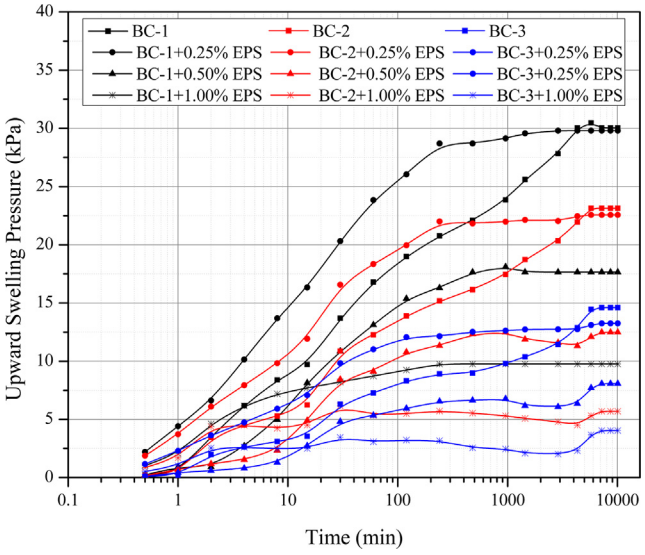

Fig. 6. Upward swelling pressure curve of reinforced and unreinforced expansive soil.

can be due to EPS beads replacing the expansive soil and consequently a reduction in the specific surface area of the swelling fraction. It also depicts that the swelling pressure of the reinforced and unreinforced expansive clayey soil changes at an exponential rate till 120 min and thereby gradually becomes constant due to saturation.

Fig. 7 shows the maximum expansion percentage of reinforced and unreinforced expansive soil. The maximum expansion percentage is defined as the ratio of the change in the vertical height of the test specimen to its original vertical height, expressed as a percentage. The 0.25% EPS and 0.50% EPS content showed higher potential in the heave reduction, as shown in Table 3. At the lower concentration of EPS content, beads get evenly distributed in the clay mix and reduce the specific surface area of hydrophobic clay minerals. Due to a reduction in the specific surface area, the expansive nature of the reinforced soil specimens con-

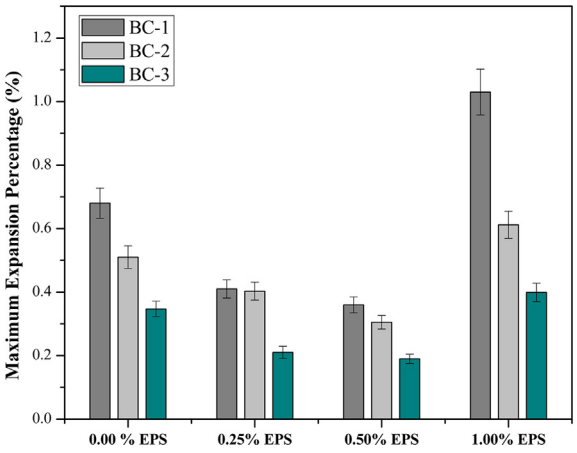

Fig. 7. Maximum expansion percentage of reinforced and unreinforced expansive soil.

Table 3
Swelling pressure and UCS results for reinforced and unreinforced expansive soils.

Soil specimen Type	Axial Strain (%)	Axial Stress (kPa)	Swelling pressure (kPa)	Expansion percentage (%)
BC-1	4.61	139.46	30.03	0.68
BC-1 + 0.25% EPS	4.61	131.21	29.80	0.41
BC-1 + 0.50% EPS	3.86	252.61	17.65	0.36
BC-1 + 1.00% EPS	4.12	105.68	9.75	1.03
BC-2	4.40	286.61	23.14	0.51
BC-2 + 0.25% EPS	5.61	474.42	22.56	0.40
BC-2 + 0.50% EPS	3.25	563.06	12.49	0.30
BC-2 + 1.00% EPS	5.18	376.21	5.70	0.61
BC-3	4.75	184.77	14.61	0.35
BC-3 + 0.25% EPS	6.83	303.97	13.25	0.21
BC-3 + 0.50% EPS	3.92	381.23	8.08	0.19
BC-3 + 1.00% EPS	5.62	357.84	4.04	0.40

trolled. However, the maximum expansion percentage in all three types of soil is observed with EPS content of 1%. At higher concentrations, the cluster formation due to EPS-EPS interaction is increasing the pore space, creating a permeable path, thereby increasing the water infiltration rate. The surplus moisture content allows more cations absorbance by hydrophobic clay mineral than the unreinforced specimen. As a result, a higher expansion percentage with a low swelling pressure has been observed with the inclusion of 1% EPS in soil.

Fig. 8 depicts the expansion percentage curve of reinforced and unreinforced expansive clayey soils. It shows that initially, the expansion in clay and EPS rises exponentially, however after 30 min, it does not show any major change in the expansion/min. During the initial process, soil specimen has air voids, and upon filling with water, it develops pore pressure. As a result, the volume changes rapidly; however, after reaching the brink of saturation limit, the expansion was minimal.

It can be ascertained that expansive soil absorbs water, and upon saturation, changes in swelling ratio without pressure can be roughly divided into three stages: (1) rapid expansion period. In general, this stage will be finished in 30 min after the expansive soil absorbs water, and the swelling amount accounts for about 60% – 80% of the total. (2) Slow expansion period. In this stage, the expansion rate is slow compared to rapid expansion and will be finished in about 20 h. (3) Stable expansion period. After expansive soil absorbs water and becomes saturated, its density is less, and the space between the soil enlarges. The time taken by the water to fill the space is more, so the expansion period lasts longer. However, these changes are slightly low; hence the curve shown in Fig. 8 is relatively stable.

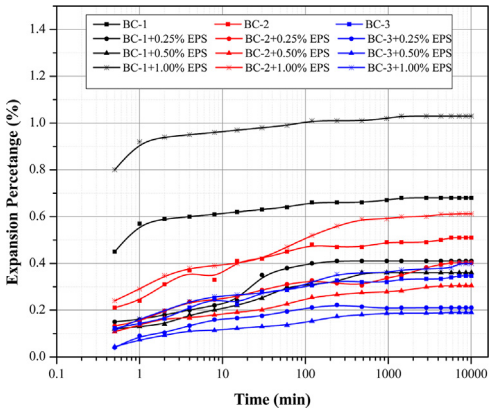

Fig. 8. Expansion percentage curve of reinforced and unreinforced expansive soil.

Fig. 9 shows the upward swelling pressure and expansion percentage ratio of reinforced and unreinforced expansive clayey soils. The upward swelling pressure and expansion percentage ratio have been calculated as per Eqs. (1) and (2).

$$\text{Upwards swelling pressure ratio} = \frac{SP_{reinforced}}{SP_{unreinforced}} \quad (1)$$

where $SP_{reinforced}$ is swelling pressure of reinforced section and $SP_{unreinforced}$ is swelling pressure of unreinforced section

$$\text{Expansion percentage ratio} = \frac{EP_{reinforced}}{EP_{unreinforced}} \quad (2)$$

where $EP_{reinforced}$ is expansion percentage of a reinforced section, and $EP_{unreinforced}$ is the expansion percentage of the unreinforced section

The plot is used to present clear changes in terms of ratio for a better understanding of swelling pressure and percentage expansion reduction. It can be noted that the upward swelling pressure ratio is observed as 0.32, 0.25, and 0.28 for the BC-1, BC-2, and BC -3, respectively, at 1% EPS content, which shows an exponential reduction in the swelling pressure. However, the values of expansion percentage ratio of 1.52, 1.2, 1.15 observed for the BC-1, BC-2, and BC -3, respectively, at 1% EPS content. The results show that the expansion percentage increase with the addition of a higher amount of EPS content, and hence 1% EPS content is not feasible for the field practices. The higher EPS content created a cluster in the soil specimen, and upon water saturation, EPS beads slide on each other and major change in the expansion percentage observed. The clustered

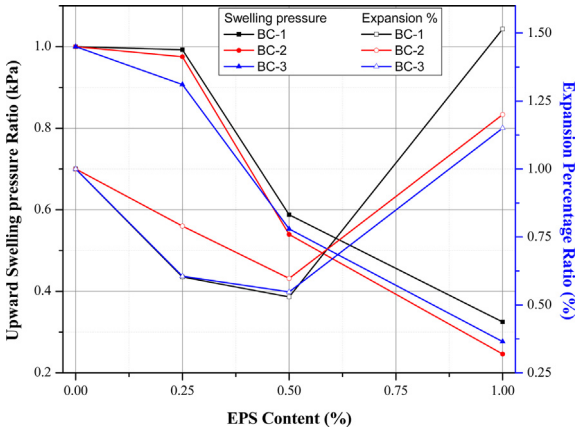

Fig. 9. Upward pressure and expansion percentage ratio of reinforced and unreinforced expansive soil.

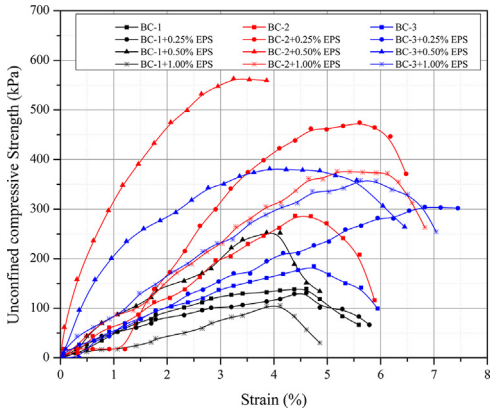

Fig. 10. Unconfined compressive strength curve of reinforced and unreinforced expansive soil.

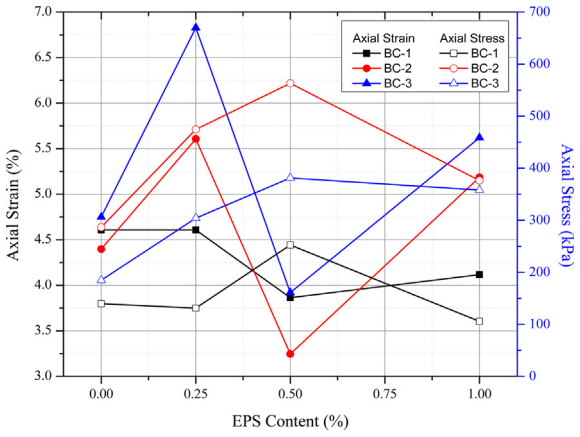

Fig. 11. Axial Stress Strain of reinforced and unreinforced expansive soil.

EPS for 1% concentration can even be observed in the UCS specimens, as shown in Fig. 4. It can also be noted that the expansion percentage reduces exponentially with the inclusion of 0.5% EPS content in expansive soil.

The axial stress-strain curve of reinforced and reinforced expansive clayey soils is shown in Fig. 10. A similar stress curve shape is observed in most cases, and the clay reaches the peak values at relatively large strains. Furthermore, it can also be noted that the 1% EPS shows a large reduction in axial strain; however, it performed better than the clay soil in terms of axial stress. This reduction can be explained as the soil grains are intact and can take care of loading through the rearrangement of voids within the soil mass. However, EPS compressive strength at a density of 21.6 kg/m^3 is around 50 kPa. Hence as the loading is increased, EPS bead compresses along with the rearrangement of soil particles, thereby decreasing the deviator strain. It is also observed that 0.5% of EPS inclusion gives higher unconfined compressive strength and is more ductile in nature (see Fig. 11).

The axial stress-strain curve for the reinforced and unreinforced expansive clayed soils with varying percentages of EPS beads are shown in Fig. 10. The unconfined compressive strength of the Soil-EPS mix increased with the increment of the EPS content; however, at a higher amount of EPS content, the axial strain capacity of the expansive soil reduces. It can be noted that 0.50% of EPSC shows a higher potential to increase the strength along with sustaining the load for large axial strain.

5. Conclusions

The results of the study on the potential use of expanded polystyrene beads to reduce the shrink-swell potential of expansive soils are presented. The use of lightweight EPS bead shows significant improvement in the engineering properties of the expansive clay soil. The modified reconstituted soils of different percentages of EPS can be used for controlling the swelling-shrinkage nature of the expansive soil subgrade. Based on the results and discussion presented, the following conclusions can be made:

1. The expansive soil reinforced with 0.5% EPS exhibited the higher unconfined compressive strength and gave an exponential reduction in the upward swelling pressure and heave.
2. The expansive soil reinforced with 0.5% EPS shows a 67–72% reduction in the swelling pressure and a 40–47% reduction in the expansion percentage. This percentage should be used as the optimum percentage for the field applications.
3. The presence of clay minerals, mainly montmorillonite, is responsible for the higher expansion. However, the inclusion of EPS bead reduces the specific surface area of swelling fraction, and as a result, reduced swelling pressure and heave are observed.

References

Al-Rawas, A.A., Hago, A.W., Al-Sarmi, H., 2005. Effect of lime, cement and Sarooj (artificial pozzolan) on the swelling potential of an expansive soil from Oman. Build. Environ. 40, 681–687. https://doi.org/10.1016/j.buildenv.2004.08.028.

Akay, O., Özer, A.T., Fox, G.A., Bartlett, S.F., Arellano, D., 2013. Behavior of sandy slopes remediated by EPS-block geofoam under seepage flow. Geotext. Geomembr. 37, 81–98. https://doi.org/10.1016/j.geotexmem.2013.02.005.

Alvarez-Puebla, R.A., Dos Santos, D.S., Blanco, C., Echeverria, J.C., Garrido, J.J., 2005. Particle and surface characterization of a natural illite and study of its copper retention. J. Colloid Interface Sci. 285, 41–49. https://doi.org/10.1016/j.jcis.2004.11.044.

Arellano, D., Stark, T.D., n.d., June 2011 Overview of NCHRP Design Guideline for EPS-Block Geofoam in Slope Stabilization and Repair. In: 4th International Conference on Geofoam Blocks in Construction Applications (EPS 2011 Norway).

Atahu, M.K., Saathoff, F., Gebissa, A., 2019. Strength and compressibility behaviors of expansive soil treated with coffee husk ash. J. Rock Mech. Geotech. Eng. https://doi.org/10.1016/j.jrmge.2018.11.004.

Aytekin, M., 1997a. Numerical modeling of EPS geofoam used with swelling soil. Geotext. Geomembr. 15, 133–146. https://doi.org/10.1016/S0266-1144(97)00010-1.

Bekhiti, M., Trouzine, H., Rabehi, M., 2019. Influence of waste tire rubber fibers on swelling behavior, unconfined compressive strength and ductility of cement stabilized bentonite clay soil. Constr. Build. Mater. 208, 304–313. https://doi.org/10.1016/j.conbuildmat.2019.03.011.

Beju, Y.Z., Mandal, J.N., 2017. Expanded Polystyrene (EPS) geofoam: preliminary characteristic evaluation. Proc. Eng. 189, 239–246. https://doi.org/10.1016/j.proeng.2017.05.038.

Christelle, B., 2005. Contribution À L'Étude De L'Activation Thermique Du Kaolin. Évolution De La Structure Cristallographique Et Activité Pouzzolanique, 96–98.

Corey, A.T., 2010. Measurement of water and air permeability in unsaturated soil. Soil Sci. Soc. Am. J. 21, 7. https://doi.org/10.2136/sssaj1957.03615995002100010003x.

Criado, M., Fernández-Jiménez, A., Palomo, A., 2007. Alkali activation of fly ash: effect of the SiO2/Na2O ratio. Micropor. Mesopor. Mater. 106, 180–191. https://doi.org/10.1016/j.micromeso.2007.02.055.

Elsharief, A.M., Zumrawi, M.M.E., Salam, A.M., 2014. Experimental Study of Some Factors Affecting Swelling Pressure 4, 4–9.

Estabragh, A.R., Rafatjo, H., Javadi, A.A., 2014. Treatment of an expansive soil by mechanical and chemical techniques. Geosynth. Int. 21, 233–243. https://doi.org/10.1680/gein.14.00011.

Farmer, V.C., n.d. The Layer Silicates 1974. In: The Infrared Spectra of Minerals. Mineralogical Society of Great Britain and Ireland, London, pp. 331–363. 10.1180/mono-4.15.

Ghani, A.N.A., Ahmad, F., Hamir, R., 2005. Development of pre-engineered geomaterial for use in road embankment and retaining structure backfill development of pre-engineered geomaterial for use in road embankment and retaining structure backfill. J. Transport. Sci. Soc. Malaysia 1.

Horvath, J.S., 1994. Expanded Polystyrene (EPS) Geofoam: an introduction to material behaviour, vol. 13, pp. 263–280.

Inoue, A., Sciences, E., Hampshire, N., 1986. morphology of Clay Minerals in the Smectite-To-Illite conversion Series By scanning electronic microscopy. Clays Clay Miner. 34, 187–197.

IS: 2720 (Part 41-1977) Indian Standards: Methods of test for soils, Part 41: Measurement of swelling pressure of soils, 1977.

IS:2720-1, 1983. Indian Standards, Methods of Test for Soils, Part 1: Preparation of dry soil samples for various tests. Indian Stand. Institutions Reaffirmed.

Karimpour-fard, M., Chenari, R.J., 2015. Shear Strength Characteristics of Sand Mixed with Eps Beads Using Large direct shear apparatus. Electron. J. Geotech. Eng. 34, 2205–2220.

Khosrowshahi, S.K.. A.S., Yildirim, H., 2014. Improvement of Expansive Soils Using Fiber Materials. p. 2014.

Liu, H., Deng, A., Chu, J., 2006. Effect of different mixing ratios of polystyrene pre-puff beads and cement on the mechanical behaviour of lightweight fill, vol. 24, pp. 331–338. 10.1016/j.geotexmem.2006.05.002.

Mackenzie, R., 1957. The differential thermal investigation of clays. Mineralogical Society (Clay Minerals Group), London.

MORTH (2019). Basic road statistics of India 2015-16 . Ministry Road transportation Highway MORTH), New Delhi India. <www.morth.nic.in>, accessed 24/04/2019.

Mirzababaei, M., Yasrobi, S., Al-Rawas, A., 2009. Effect of polymers on swelling potential of expansive soils. Proc. Inst. Civ. Eng. - Gr. Improv. 162, 111–119. https://doi.org/10.1680/grim.2009.162.3.111.

Mustafa Aytekin, June 1997. Numerical Modeling of EPS geofoam used with swelling soil. Geotext. Geomembr. 10.1016/S0266-1144(97)00010-1.

Nelson, D., Miller, D.J., 1993. Book review expansive soils-problems and practice in foundation and pavement engineering:, vol. 17, pp. 745–746.

Öncü, Ş., Bilsel, H., 2017. Effect of zeolite utilization on volume change and strength properties of expansive soil as landfill barrier. Can. Geotech. J. 54, 1320–1330. https://doi.org/10.1139/cgj-2016-0483.

Petit, S., Madejova, J., Decarreau, A., Martin, F., Poitiers, U. De, A, U. M.R.C.H.A.S., Cedex, F.-P., 1999. Kaolinites Using Near Infrared Spectroscopy. Clays Clay Miner., vol. 47, pp. 103–108.

Phanikumar, B.R., Singla, R., 2016. Swell-consolidation characteristics of fibre-reinforced expansive soils. Soils Found. 56, 138–143. https://doi.org/10.1016/j.sandf.2016.01.011.

Prusty, J.K., Patro, S.K., 2015. Properties of fresh and hardened concrete using agro-waste as partial replacement of coarse aggregate - a review. Constr. Build. Mater. 10.1016/j.conbuildmat.2015.02.063.

Puppala, A.J., Punthutaecha, K., Vanapalli, S.K., 2006. Soil-water characteristic curves of stabilized expansive soils. J. Geotech. Geoenviron. Eng. 132, 736–751. https://doi.org/10.1061/(ASCE)1090-0241(2006)132:6(736).

Rao, a V.N., Chittaranjan, M., Lecturer, S., District, G., 2001. Study on performance of chemically stabilized expansive soil. Int. J. Adv. Eng. Technol. 5, 32–37.

Robertson, A.H.J., Hill, H.R., Main, A.M., 2013. Analysis of Soil in the Field using portable FTIR. Soil Spectrosc.: Present Future Soil Monitor., 1–20

Senol, A., Khosrowshahi, S.K.., Yildirim, H.., 2014. Improvement of Expansive Soils Using Fiber Materials. In: The 11th International Congress on Advances in Civil Engineering (ACE 2014). Istanbul, Turkey.

Shi, B., Wu, Z., Inyang, H., Chen, J., Wang, B., 1999. Preparation of soil specimens for SEM analysis using freeze-cut-drying. Bull. Eng. Geol. Environ. 58, 1–7. https://doi.org/10.1007/s100640050064.

Shelke, A.P., Murthy, D.S., 2010. Reduction of Swelling Pressure of Expansive Soils Using EPS Geofoam. In: Proc. Indian Geotech. Conf. 2010 GEOtrendz, December 16–18 495–498.

Sivakumar Babu, G.L., Vasudevan, A.K., Haldar, S., 2008. Numerical simulation of fiber-reinforced sand behavior. Geotext. Geomembr. 26, 181–188. https://doi.org/10.1016/j.geotexmem.2007.06.004.

Soundara, B., Robinson, R.G., 2009. Influence of test method on swelling pressure of compacted clay. Int. J. Geotech. Eng. 3, 439–444. https://doi.org/10.3328/IJGE.2009.03.03.439-444.

Srinivas, K., Prasad, D.S.V., Rao, E.V.K.L., 2016. A study on improvement of expansive soil by using Cns (Cohesive Non Swelling) Layer. Int. J. Innov. Res. Technol. 3, 54–60.

Srivastava, D.K., Srivastava, A., Misra, A.K., Sahu, V., 2018. Sustainability assessment of EPS-geofoam in road construction: a case study. Int. J. Sustain. Eng. 1–8. https://doi.org/10.1080/19397038.2018.1508319.

Tatsuoka, F., Correia, A.G., 2016. Importance of controlling the degree of saturation in soil compaction. Proc. Eng. 143, 556–565. https://doi.org/10.1016/j.proeng.2016.06.070.

Tiwari, N., Satyam, N., 2019. Experimental study on the influence of polypropylene fiber on the swelling pressure expansion attributes of silica fume stabilized clayey soil. Geosciences 9, 377. https://doi.org/10.3390/GEOSCIENCES9090377.

Tiwari, N., Satyam, N., 2020. An experimental study on the behavior of lime and silica fume treated coir geotextile reinforced expansive soil subgrade. Eng. Sci. Technol. an Int. J. 10.1016/j.jestch.2019.12.006.

Yazdandoust, F., Yasrobi, S.S., 2010. Effect of cyclic wetting and drying on swelling behavior of polymer-stabilized expansive clays. Appl. Clay Sci. 50, 461–468. https://doi.org/10.1016/j.clay.2010.09.006.

Yoonz, Gil-lim, Jeon, Sang-soo, Kim, Byung-tak, Kim, Byung-tak, 2014. Mechanical characteristics of light- weighted soils using dredged

materials mechanical characteristics of light-weighted soils using dredged materials, 37–41. 10.1080/10641190490467747.
WHO (2018). World Health Statistics, 2018, World Health organization (WHO), 10.22201/fq.18708404e.2004.3.66178, 5-13.
Zarnani, S., Bathurst, R.J., 2007. Experimental investigation of EPS geofoam seismic buffers using shaking table tests. 10.1680/gein.2007.14.3.165.
Zhou, Y., Li, M., He, Q., Wen, K., 2018. Deformation and damping characteristics of lightweight clay-EPS soil under cyclic loading. Adv. Civ. Eng. 2018, 1–10. https://doi.org/10.1155/2018/8093719.